Thermal conductivity of pillared graphene-epoxy nanocomposites using molecular dynamics

A. Lakshmanan, S. Srivastava, A. Ramazani,[a] and V. Sundararaghavan[b]
Department of Aerospace Engineering, University of Michigan, Ann Arbor, Michigan 48109, USA

(Received 18 January 2018; accepted 26 March 2018; published online 9 April 2018)

Thermal conductivity in a pillared graphene-epoxy nanocomposite (PGEN) is studied using equilibrium molecular dynamics simulations. PGEN is a proposed material for advanced thermal management applications because it combines high in-plane conductivity of graphene with high axial conductivity of a nanotube to significantly enhance the overall conductivity of the epoxy matrix material. Anisotropic conductivity of PGEN has been compared with that of pristine and functionalized carbon nanotube-epoxy nanocomposites, showcasing the advantages of the unique hierarchical structure of PGEN. Compared to pure carbon allotropes, embedding the epoxy matrix also promotes a weaker dependence of conductivity on thermal variations. These features make this an attractive material for thermal management applications. *Published by AIP Publishing.*
https://doi.org/10.1063/1.5022755

Owing to their high specific strength, high specific stiffness, fatigue resistance, and ease of manufacturing, polymer-matrix composites have been widely used in aerospace, automotive, marine, and other applications involving high performance requirements.[1] Specifically, epoxies are preferred for aerospace grade components due to their superior mechanical properties and desirable resistance to moisture-induced degradation. However, their low thermal conductivity of 0.1–0.2 W/mK (Ref. 2) limits their use to low temperature applications. Subsequent attempts involved enhancing the conductivity and other thermomechanical properties through the addition of various high-conductivity fillers[3–9] in different proportions to achieve a maximum of about 4.5 W/mK which is still insufficient.

In order to overcome this shortcoming, attention was shifted to include graphene-based additives exhibiting high thermal conductivity, desirable mechanical characteristics, and tunability. The measured value of in-plane thermal conductivity of graphene was shown to reach as high as several thousands of watt per meter Kelvin,[10–13] among the highest values of known materials. Similarly, the axial thermal conductivity of carbon nanotubes (CNTs) exceeded a few thousands of watts per meter Kelvin,[14–16] which could be modified through changes in their length, diameter, chirality, number of lateral walls, and functionalization. Consequently, graphene-epoxy composites[17–23] and carbon nanotube (CNT)-epoxy composites[24–28] have been a subject of extensive research in the past decade.

Graphene and CNTs, however, exhibit significant anisotropy with relatively high thermal conductivity in the planar and axial directions, respectively.[29–31] As a result, when these allotropes (CNT/graphite) are introduced as fillers/additives in polymer composites, only a minor enhancement is observed in the effective value of thermal conductivity. As these fillers are randomly dispersed in the matrix, they almost always come in transverse contact over a relatively less contact area, leading to very high thermal resistivity,[24] suggesting the use of three-dimensional architectures as fillers like pillared-graphene (PG). Several recent experimental efforts have aimed at realizing these hierarchical structures in the laboratory.[32–38]

The technique of non-equilibrium molecular dynamics has been employed to compute the thermal conductivity of pillared graphene architectures.[39–41] Their studies on the dependence of conductivity on the interpillar distance, pillar height, and CNT-graphene junction defects predicted that for the same pillar height and interpillar distance, the in-plane thermal conductivity was higher than the out-of-plane thermal conductivity due to the anisotropy of the structure. The thermal conductivity and interfacial thermal resistance of a PG architecture were investigated for two different junction types, pure sp^2 hybridized and mixed sp^2/sp^3 hybridized,[42] recording a 25 percent decrease in out-of-plane thermal conductivity of both the PG architectures as compared to a CNT. This was attributed to the junction defects as also computed using a resistance model[43] and phonon scattering studies.[44] However, compared to few layer graphene, it was found that Graphene-CNT hybrid structures significantly enhanced the phonon transmission in the out-of-plane direction.[45] All these studies point to the fact that the thermal conductivity of the conventional epoxy matrix materials can be enhanced by curing it along with 3D architectured additives in comparison to 1D (CNT) or 2D (graphene) additives alone. However, the effect of the epoxy matrix interspersed in these pillared architectures has not been simulated in these works. In addition, the effect of temperature on the thermal conductivity in such structures has not yet been studied, which would correspond to the realistic scenarios in which these thermal management devices would operate.

In this communication, we present the thermal conductivity estimates for a pillared graphene-epoxy nanocomposite (PGEN). Previous attempts using NEMD furnished only a single scalar measure of thermal conductivity, and temperature dependence assessment of the conductivity is non-trivial

[a]Present address: Department of Mechanical Engineering, Massachusetts Institute of Technology, Cambridge, Massachusetts 02139, USA.
[b]Electronic mail: veeras@umich.edu. Tel.: +1 (734) 615-7242.

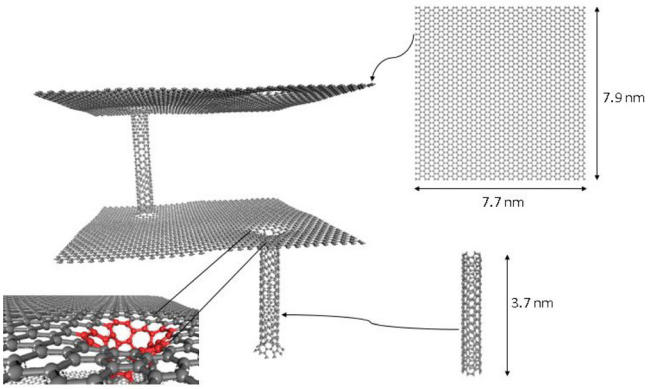

FIG. 1. Aerographene assembled using graphene and SWCNT.

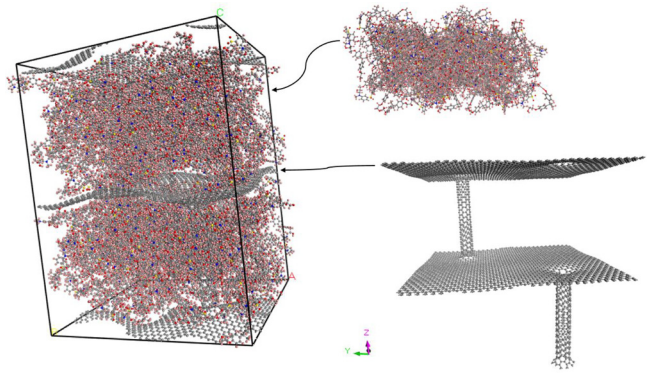

FIG. 2. PGEN assembled using epoxy and aerographene. Blue—Nitrogen, Red—Oxygen, and Yellow—Sulphur.

due to the existing heterogeneous temperature distribution during the simulation. We instead resort to a combination of classical results from linear response theory and equilibrium molecular dynamics simulations to estimate the anisotropic thermal conductivity of PGEN and compare the results with SWCNT-reinforced epoxy nanocomposites.[46–48] Although this approach is a very general one, it must be used with some care to obtain satisfactorily accurate results.[49–51] This is the first study to use equilibrium molecular dynamics simulations to compute the thermal conductivity of architectured nanocomposites.

The PGEN structure comprises 3 main components: graphene, CNT, and epoxy. The structure was constructed in Materials Studio 8^{TM} and exported as a Consistent Valence Force Field (CVFF) potential file. The non-bonded interactions were captured in the form of two potential contributions: (i) LJ potential and (ii) Coulombic pairwise interactions with a cut-off. Diglycidyl ether of bisphenol A (DGEBA) crosslinked with curing agent 3–3 diamino diphenyl sulfone (DDS) was the epoxy chosen for this study. A dendrimer approach was utilized to expand the network, followed by an annealing procedure (Ref. 52, also see supplementary material) to increase the density of the system closer to the experimental value. The converged density of epoxy was found to be 1.77 g/cc at 1 K and 1 atm pressure. Then, a SWCNT[47] (4,4) was inserted after creating a vacancy in the epoxy by moving atoms radially outward at $\frac{1}{4}$ th and $\frac{3}{4}$ th of the length along the diagonal. The annealing procedure was repeated to equilibrate the structure followed by the build layer procedure to create a periodic simulation cell made of two alternating layers of graphene and CNT-epoxy, with CNTs arranged on alternating diagonals of the sheet. Creation of bonds between the CNT and graphene resulted in the presence of Stone-Wales defects at the junction (marked red in Fig. 1). The PGEN structure was then equilibrated on a periodic triclinic cell until a converged value of the density was obtained. The final structure had 3.53% mass fraction of CNT and comprised 41872 atoms with 288 amine groups and 568 epoxy groups. The triclinic cell was $76.38 \times 78.35 \times 75.47$ Å^3, with angles of 99.6°, 90.8°, and 90.0°. The pillared graphene and PGEN are depicted in Figs. 1 and 2, respectively, accompanied by the basic structures used to construct it. The estimates for thermal conductivity for the PGEN are compared with those of SWCNT-epoxy composites reported earlier[46] in which the same epoxy chemistry, epoxy to amine ratio, force fields, nanotube chirality, and cross-link conversion were used.

Equilibrium molecular dynamics simulations were performed using LAMMPS[53] based on the Green-Kubo[54] expression which relates the thermal conductivity tensor to the integral over time t of the heat flux autocorrelation function as follows:

$$\boldsymbol{\kappa} = \frac{1}{Vk_BT^2}\int_0^\infty < \mathbf{J}(t) \otimes \mathbf{J}(0) > dt. \tag{1}$$

V is the volume of the unit cell, k_B Boltzmann's constant, T the temperature, $\mathbf{J}$ the atomistic heat flux vector, and $\otimes$ the dyadic product of vectors. The ensemble averaging and computation of the integral in (1) were approximated numerically using trapezoidal integration, with a correlation length of 20 ps and a sampling time of 10 ns, with a sampling interval of 1 fs. Periodic boundary conditions were imposed in all directions. The PGEN structure was first equilibrated using the NPT ensemble for 2 ns, at the desired temperature and 1 atm pressure. The next 10 ns correspond to the sampling time during which the heat flux vector was calculated from the per atom kinetic energy, potential energy, and virial stress. The average correlation of the heat flux was then computed every 20 ps, which is then used to calculate the thermal conductivity tensor. For the case of SWCNT-epoxy nanocomposites as in Ref. 46, the structures were equilibrated at the temperature being studied for 0.5 ns, followed by further equilibration and collection of heat current data used for the calculation of the autocorrelation function. A correlation time of 16 ps was used with a sampling time of 1.6 ns and a sampling interval of 1 fs. We had to use longer correlation times and correspondingly longer sampling times due to the complexity of the system, arising from its size.

It is very important to note that the approach of equilibrium molecular dynamics combined with the Green-Kubo relations provides an efficient way to estimate the properties of tensorial nature through just a single simulation. This makes the approach extremely efficient as compared to the existing NEMD techniques which furnish only a scalar (unidirectional) measure of the property per simulation.

The diagonal components of the thermal conductivity tensor are reported and compared with SWCNT-epoxy and pure epoxy system estimates from the literature. Table I reports the ratio of the thermal conductivity of the three

TABLE I. Thermal conductivity comparison relative to neat epoxy.

Ratio w.r.t epoxy	PGEN MD	Pristine SWCNT-epoxy		Functionalized SWCNT-epoxy	Contiguous–SWCNT-epoxy
		MD[46]	Exp.[25]	MD[46]	MD[46]
κ_{xx}	131.04	0.99	1.0	1.50	0.87
κ_{yy}	145.95	0.99	1.0	1.50	0.87
κ_{zz}	12.63	2.21	2.26	2.12	166.0

carbon-based epoxy systems relative to the pure epoxy at 300 K. The MD and experimental values were normalized with respect to those of neat epoxy from MD simulations and experiments, respectively. Discontinuous SWCNT-epoxy was used for comparison because experimental preparation results in the formation of broken CNTs in the epoxy matrix. Referring to Table I and Fig. 3, it is found that the off-axis (or in-plane) thermal conductivity of PGEN clearly overshadows that of its counterparts by at least two orders of magnitude. The high relative conductivity along the x and y directions can be attributed to the graphene sheet with defects which dominates the in-plane conductivity. In contrast, the thermal conductivity of the structures possessing only CNTs is dictated almost completely by the epoxy which has much lower thermal conductivity compared to graphene. Conductivity of CNT-epoxy composites is found to increase with functionalization of CNT with epoxy, which is still not as high as the PGEN.

For thermal conductivity along the CNT axis, it was observed again that the PGEN dominates over the other nanocomposites. This is attributed to the PG forming a fully connected network, providing an alternate path for heat transmission. Discontinuous (pristine and functionalized) SWCNT-epoxy nanocomposites are able to achieve only a slight enhancement in conductivity along z with respect to pure epoxy due to the lack of continuity of the CNTs and moreover due to the intermediate epoxy impeding the transmission of heat. It is noted that the thermal conductivity enhancement in the z-direction of PGEN (12.63×) over pure epoxy is lower than that obtained from a continuous (periodic) reinforcement with a nanotube (166×[46]) with the continuous reinforcement however being an idealized case. This is due to unavailability of a direct defect free-path in the z-direction in PGEN due to Stone–Wales defects present at the CNT-graphene junction. Additionally, a lower CNT mass fraction of 3.53% in PGEN results in a higher value of thermal conductivity as compared to the discontinuous SWCNT-epoxy composite at a mass fraction of 6%.

Figures 4 and 5 depict the comparison of the conductivity components for the PGEN with those of pyrolytic graphite,[55] (10,10) SWCNT,[29] pristine (Prstn), and functionalized (Fnc) SWCNT-epoxy nanocomposite.[46] It is already known that graphene and SWCNT exhibit highly anisotropic thermal conductivity. The in-plane conductivity for graphene can be almost five orders of magnitude higher than its out-of-plane component. The same is true for SWCNT when we compare the axial component with the transverse component. Neat epoxy on the other hand depicts extremely low, isotropic conductivity. The PGEN exhibits higher thermal conductivity compared to neat epoxy and simultaneously a greater extent of isotropy than its constituent carbon allotropes, which is attributed to its hierarchical structure. The arrangement of the SWCNT and graphene perpendicular to each other provides a relatively low resistance path for heat flow, which can now occur both along the axis of the SWCNT and in the plane of graphene. Moreover, the in-plane component is higher than the axial component due to the presence of an (almost) continuous graphene sheet ensuring direct connectivity unlike the vertically disconnected SWCNTs. From the point of view of temperature sensitivity, the PGEN or the SWCNT-epoxy composites show a weaker temperature dependence compared to the corresponding carbon allotropes, which can be attributed to the presence of the epoxy matrix which itself shows a weak temperature dependence.

The axial thermal conductivity of the PGEN is lower by only an order of magnitude compared to the pristine SWCNT-epoxy for which periodic boundary conditions were ensured while computing the thermal conductivity. The reduction is attributed to the presence of SWCNT-graphene junctions which act as phonon scattering centers inhibiting effective heat flow. The not-so-drastic reduction is attributed to the

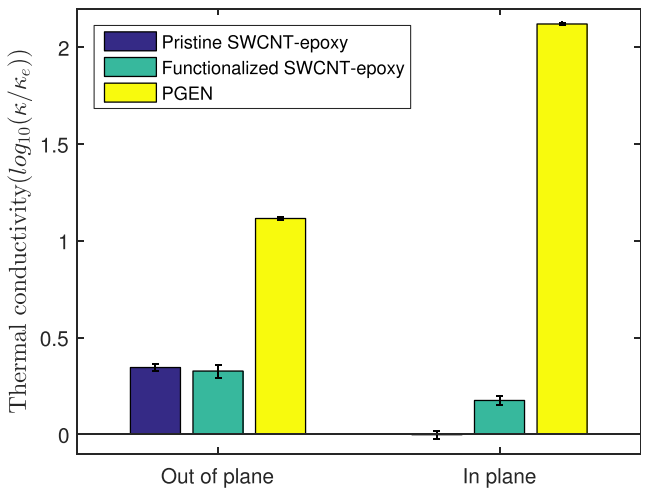

FIG. 3. Thermal conductivity comparison between different nanocomposites at 300 K normalized to the corresponding conductivity of neat epoxy.

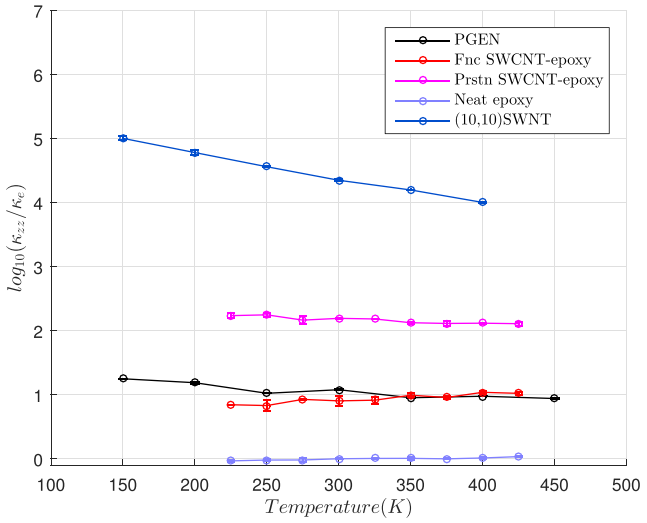

FIG. 4. Comparison of axial thermal conductivity of PGEN with that of other nanostructures.

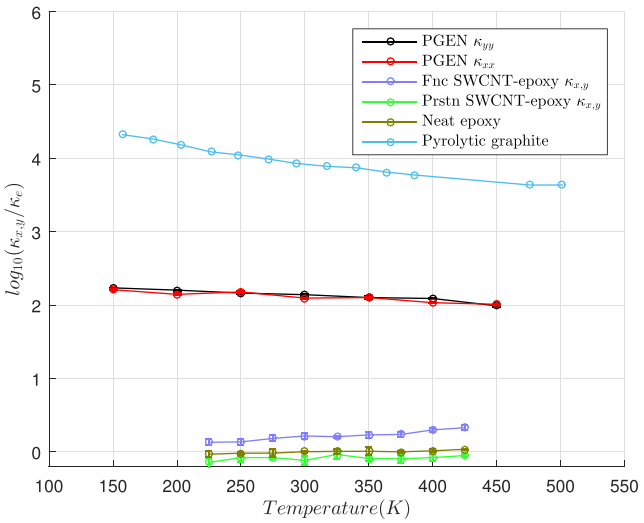

FIG. 5. Comparison of in-plane thermal conductivity of PGEN with that of other nanostructures.

SWCNT pair which are displaced with respect to each other and connected by the graphene (Fig. 1), providing a contiguous path for heat transmission. The (10,10) SWCNT exhibits a more sensitive dependence of its conductivity with temperature compared to the other two structures for which the conductivity is slowly varying in the range of 250 K–400 K.[56] At lower temperatures, however, the PGEN shows a more pronounced temperature dependence.

Functionalization brings in the effect of the epoxy in terms of a lower value of conductivity in the axial direction, but the in-plane conductivity is increased. However, PGEN dominates the in-plane conductivity due to the highly conducting graphene layer, albeit with junctions impeding phonon transmission. When we inspect the temperature dependence of the axial conductivity, the PGEN and pristine SWCNT-epoxy depict a decrease as opposed to the functionalized SWCNT-epoxy which shows an increasing trend. This is another evidence supporting the enhanced effect of the epoxy through functionalization because neat epoxy shows increasing conductivity with temperature as well. The increase in the conductivity of the epoxy with temperature is expected because it is essentially disordered where the conduction mechanism is the hopping of localized excitations coupled by harmonic forces.[57] In the case of in-plane conductivity, the SWCNT-epoxy system shows an increasing trend dictated by the behavior of the epoxy. In the case of PGEN, however, due to the intermediate graphene sheet, the in-plane conductivity reflects a temperature dependence very much like the graphene sheet itself which shows a decrease with temperature. The experimental measurements for the temperature dependent thermal conductivity of pyrolytic graphite[55] are included in Fig. 5 to reflect this trend.

Based on the above observations, we may reason that the epoxy aids in reducing the sensitivity of thermal conductivity to temperature. The PGEN is thus less sensitive to temperature changes, which is a desirable property and simultaneously supports a more effective flow of heat due to the presence of a contiguous SWCNT-graphene-SWCNT path. For any thermal management application, we would prefer that the conductivity shows an increase with temperatures primarily to facilitate faster conduction at higher working temperatures. While appropriate hierarchical structures maybe considered for enhancement in thermal conductivity, careful functionalization may aid in a positive temperature dependence for these structures, resulting in improved materials for thermal management. It would be insightful to perform a parametric study of the conductivity with respect to the parameters characterizing the hierarchical structure (pillar length, inter-pillar distance, CNT chirality, and junction characteristics), functionalization, and the imposed mechanical strain.

In conclusion, equilibrium molecular dynamics simulations have been used to estimate the anisotropic thermal conductivity of PGEN for various temperatures. The PGEN structure was formed when curing epoxy alongside a pillared graphene network. The conductivity of this structure was compared against pristine and functionalized SWCNT-epoxy nanocomposites and the constituent carbon allotropes from previous works. The relatively high overall conductivity of PGEN compared to that of the other nanocomposites was related to its hierarchical structure which provides alternate pathways for the conduction of heat. Further, the temperature dependence was also compared qualitatively with carbon allotropes and carbon based nanocomposites to drive the point that PGEN achieved the balance of satisfactory thermal conductivity and temperature sensitivity, justifying the need for further research into these materials as thermal management materials.

See supplementary material for the annealing protocol and thermal conductivity convergence in the Green Kubo calculations.

[1]R. E. Shalin, *Polymer Matrix Composites* (Springer Science & Business Media, 2012), Vol. 4.
[2]F. De Araujo and H. Rosenberg, J. Phys. D: Appl. Phys. **9**, 665 (1976).
[3]P. Bujard and J. Ansermet, in *Fifth Annual IEEE Semiconductor Thermal and Temperature Measurement Symposium* (1989), Vol. 126.
[4]P. Procter and J. Solc, IEEE Trans. Compon., Hybrids, Manuf. Technol. **14**, 708 (1991).
[5]P. Bujard, in *InterSociety Conference on Thermal Phenomena in the Fabrication and Operation of Electronic Components: I-THERM '88* (1988), p. 41.
[6]G. W. Lee, M. Park, J. Kim, J. I. Lee, and H. G. Yoon, Compos. Part A: Appl. Sci. Manuf. **37**, 727 (2006).
[7]K. W. Garrett and H. M. Rosenberg, J. Phys. D: Appl. Phys. **7**, 1247 (1974).
[8]S. Ino and T. Shiobara, IEEE Trans. Compon. Packag. Manuf. Technol. Part A **17**, 527 (1994).
[9]C. P. Wong and R. S. Bollampally, J. Appl. Polym. Sci. **74**, 3396 (1999).
[10]A. Balandin, S. Ghosh, W. Bao, I. Calizo, D. Teweldebrhan, F. Miao, and C. N. Lau, Nano Lett. **8**, 902 (2008).
[11]L. A. Jauregui, Y. Yue, A. N. Sidorov, J. Hu, Q. Yu, G. Lopez, R. Jalilian, D. K. Benjamin, D. A. Delkd, W. Wu, Z. Liu, X. Wang, Z. Jiang, X. Ruan, J. Bao, S. S. Pei, and Y. P. Chen, ECS Trans. **28**, 73 (2010).
[12]C. Faugeras, B. Faugeras, M. Orlita, M. Potemski, R. R. Nair, and A. K. Geim, ACS Nano **4**, 1889 (2010).
[13]W. Cai, A. L. Moore, Y. Zhu, X. Li, S. Chen, L. Shi, and R. S. Ruoff, Nano Lett. **10**, 1645 (2010).
[14]T.-Y. Choi, D. Poulikakos, J. Tharian, and U. Sennhauser, Nano Lett. **6**, 1589 (2006).
[15]P. Kim, L. Shi, A. Majumdar, and P. L. McEuen, Phys. Rev. Lett. **87**, 215502 (2001).
[16]M. Fujii, X. Zhang, H. Xie, H. Ago, K. Takahashi, T. Ikuta, H. Abe, and T. Shimizu, Phys. Rev. Lett. **95**, 065502 (2005).
[17]B. Mortazavi, O. Benzerara, H. Meyer, J. Bardon, and S. Ahzi, Carbon **60**, 356 (2013).

[18]S. H. Song, K. H. Park, B. H. Kim, Y. W. Choi, G. H. Jun, D. J. Lee, B. S. Kong, K. W. Paik, and S. Jeon, Adv. Mater. **25**, 732 (2013).
[19]C. C. Teng, C. C. M. Ma, C. H. Lu, S. Y. Yang, S. H. Lee, M. C. Hsiao, M. Y. Yen, K. C. Chiou, and T. M. Lee, Carbon **49**, 5107 (2011).
[20]K. M. F. Shahil and A. Balandin, Nano Lett. **12**, 861–867 (2012).
[21]K. M. Shahil and A. A. Balandin, Solid State Commun. **152**, 1331 (2012).
[22]R. Verdejo, M. M. Bernal, L. J. Romasanta, and M. A. Lopez-Manchado, J. Mater. Chem. **21**, 3301 (2011).
[23]J. Renteria, S. Legedza, R. Salgado, M. Balandin, S. Ramirez, M. Saadah, F. Kargar, and A. Balandin, Mater. Des. **88**, 214 (2015).
[24]M. J. Biercuk, M. C. Llaguno, M. Radosavljevic, J. K. Hyun, A. T. Johnson, and J. E. Fischer, Appl. Phys. Lett. **80**, 2767 (2002).
[25]M. B. Bryning, D. E. Milkie, M. F. Islam, J. M. Kikkawa, and A. G. Yodh, Appl. Phys. Lett. **87**, 161909 (2005).
[26]A. Moisala, Q. Li, I. A. Kinloch, and A. H. Windle, Compos. Sci. Technol. **66**, 1285 (2006).
[27]F. H. Gojny, M. H. G. Wichmann, B. Fiedler, I. A. Kinloch, W. Bauhofer, A. H. Windle, and K. Schulte, Polymer **47**, 2036 (2006).
[28]J. N. Coleman, U. Khan, W. J. Blau, and Y. K. Gunko, Carbon **44**, 1624 (2006).
[29]S. Berber, Y.-K. Kwon, and D. Tománek, Phys. Rev. Lett. **84**, 4613 (2000).
[30]B. T. Kelly, *Physics of Graphite* (Applied Science, 1981), p. 477.
[31]J. Che, T. Çagin, and W. A. Goddard, Nanotechnology **11**, 65 (2000).
[32]F. Du, D. Yu, L. Dai, S. Ganguli, V. Varshney, and A. K. Roy, Chem. Mater. **23**, 4810 (2011).
[33]R. K. Paul, M. Ghazinejad, M. Penchev, J. Lin, M. Ozkan, and C. S. Ozkan, Small **6**, 2309 (2010).
[34]Y. Zhu, L. Li, C. Zhang, G. Casillas, Z. Sun, Z. Yan, G. Ruan, Z. Peng, A.-R. O. Raji, C. Kittrell, R. H. Hauge, and J. M. Tour, Nat. Commun. **3**, 1225 (2012).
[35]M. Ghazinejad, S. Guo, W. Wang, M. Ozkan, and C. S. Ozkan, J. Mater. Res. **28**, 958 (2013).
[36]C. S. Rout, A. Kumar, T. S. Fisher, U. K. Gautam, Y. Bando, and D. Golberg, RSC Adv. **2**, 8250 (2012).
[37]L. Ruitao, C.-S. Eduardo, and T. Mauricio, ACS Nano **8**, 4061 (2014).
[38]M. Qin, Y. Feng, T. Ji, and W. Feng, Carbon **104**, 157 (2016).
[39]V. Varshney, S. S. Patnaik, A. K. Roy, G. Froudakis, and B. L. Farmer, ACS Nano **4**, 1153 (2010).
[40]J. Park and V. Prakash, in *Proceedings of the ASME 2013 International Mechanical Engineering Congress and Exposition* (2017), pp. 1–8.
[41]L. Xu, N. Wei, Y. Zheng, Z. Fan, H.-Q. Wang, and J.-C. Zheng, J. Mater. Chem. **22**, 1435 (2012).
[42]J. Park and V. Prakash, J. Mater. Res. **28**, 940 (2012).
[43]J. Shi, Y. Dong, T. Fisher, and X. Ruan, in *Proceedings of the ASME 2014 International Mechanical Engineering Congress and Exposition* (2017), pp. 1–7.
[44]J. Lee, V. Varshney, J. S. Brown, A. K. Roy, and B. L. Farmer, Appl. Phys. Lett. **100**, 183111 (2012)
[45]J. Chen, J. H. Walther, and P. Koumoutsakos, Adv. Funct. Mater. **25**, 7539 (2015).
[46]N. A. Fasanella, "Multiscale modeling of carbon nanotube-epoxy nanocomposites by," Ph.D. thesis (University of Michigan, Ann Arbor, 2016).
[47]N. A. Fasanella and V. Sundararaghavan, JOM **68**, 1396 (2016).
[48]N. Fasanella and V. Sundararaghavan, Modell. Simul. Mater. Sci. Eng. **23**, 065003 (2015).
[49]J. Chen, G. Zhang, and B. Li, Phys. Lett. A **374**, 2392 (2010).
[50]P. K. Schelling, S. R. Phillpot, and P. Keblinski, Phys. Rev. B **65**, 144306 (2002).
[51]A. Dhar, Adv. Phys. **57**, 457 (2008).
[52]V. Sundararaghavan and A. Kumar, Int. J. Plast. **47**, 111 (2013).
[53]S. Plimpton, J. Comput. Phys. **117**, 1 (1995).
[54]R. Kubo, J. Phys. Soc. Jpn. **12**, 570 (1957).
[55]A. A. Balandin, Nat. Mater. **10**, 569 (2011).
[56]J. R. Lukes and H. Zhong, J. Heat Transfer **129**, 705 (2007).
[57]D. G. Cahill and R. Pohl, Solid State Commun. **70**, 927 (1989).